THE JOURNAL OF BIOLOGICAL CHEMISTRY
Vol. 270, No. 22, Issue of June 2, pp. 13216–13224, 1995
Printed in U.S.A.

Kinetics and Thermodynamics of Virus Binding to Receptor

STUDIES WITH RHINOVIRUS, INTERCELLULAR ADHESION MOLECULE-1 (ICAM-1), AND SURFACE PLASMON RESONANCE*

(Received for publication, February 7, 1995, and in revised form, March 31, 1995)

José M. Casasnovas and Timothy A. Springer‡

From the Harvard Medical School, Department of Pathology, The Center for Blood Research, Boston, Massachusetts 02115

We have studied the kinetics and thermodynamics of a virus interacting with its receptor using human rhinovirus serotype 3 (HRV3), soluble intercellular adhesion molecule-1 (ICAM-1, CD54) containing Ig superfamily domains 1–5 (sICAM-1), and surface plasmon resonance. There were two classes of binding sites for sICAM-1 on HRV3, each comprising about 50% of the total sites, with association rate constants of 2450 ± 300 and 134 ± 11 M^{-1} s^{-1}. These rates are low, consistent with binding to a relatively inaccessible site in the rhinovirus canyon. By contrast, three monoclonal antibodies bound to sICAM-1 with a single rate constant of 17,000–48,000 M^{-1} s^{-1}. The dissociation rate constant for HRV3 was 1.7 ± 0.1 × 10^{-3} s^{-1}, giving calculated dissociation constants of 0.7 ± 0.1 and 12.5 ± 1.2 μM. Agreement was good with saturation binding in solution, which showed two sites of similar abundance with K_D of 0.55 ± 0.2 and 5.7 ± 2.0 μM. A bivalent chimera of ICAM-1 with the IgA1 Fc region bound with K_D = 50 and 410 nM, showing 17-fold enhanced affinity. Lowering pH from 8.0 to 6.0 reduced affinity by approximately 50-fold, primarily by reducing the on rate. Thermodynamic measurements showed that binding of ICAM-1 to HRV3 is endothermic, by contrast to binding to monoclonal antibody. The heat that is absorbed of 3.5 and 6.3 kcal/mol for the two classes of ICAM-1 binding sites may contribute to receptor-mediated disruption of virions, which has an activation energy of about 42 kcal/mol.

Human rhinoviruses are small, non-enveloped RNA viruses of the picornavirus family that have a capsid of icosahedral symmetry and are 300 Å in diameter (1–3). The outer part of the capsid is constructed from 60 copies of viral coat proteins VP1, VP2, and VP3; VP4 is located on the inner face of the proteinaceous capsid. It has been proposed that the receptor binding site is located in a depression or "canyon" encircling the 5-fold icosahedral vertices and that five receptor binding sites are present around each of these vertices (4). Cryoelectron microscopy, site-directed mutagenesis, and saturation binding studies have confirmed these hypotheses (5, 6, 19). The residues implicated in the interaction with the receptor are buried in the canyon, which has been hypothesized to make the receptor binding site inaccessible to antibodies and to protect the viral receptor binding site from immune surveillance (4). It may also be important that antibody binding sites have a bigger footprint than the receptor binding site (8), and thus mutations in regions outside but adjacent to the receptor binding site can contribute to the immunological diversity among serotypes without affecting receptor binding.

Intercellular adhesion molecule-1 (ICAM-1)[1] is the receptor for the major group of rhinoviruses (9–11). ICAM-1 is a membrane protein with five immunoglobulin superfamily (IgSF) extracellular domains, a hydrophobic transmembrane domain, and a short cytoplasmic domain (12, 13). ICAM-1 is the counter-receptor for the leukocyte integrins LFA-1 and Mac-1 and promotes a wide range of cell interactions important in inflammation (14). ICAM-1 is also utilized as a sequestration receptor for *Plasmodium falciparum*-infected erythrocytes (15). The binding site on ICAM-1 for rhinovirus is located primarily in the N-terminal or first IgSF domain, with perhaps some contribution from the second IgSF domain (16, 17). A recombinant soluble form of ICAM-1 truncated at the membrane that contains all five IgSF domains (sICAM-1) has been shown to inhibit rhinovirus infection (18) and induce irreversible modification of the viral capsid *in vitro* (7, 19, 20). High efficiency in rhinovirus neutralization has been obtained with multivalent ICAM-1 Ig chimeras (20).

The equilibria, kinetics, and thermodynamics of virus binding to receptors is interesting from both biological and mechanistic points of view. The affinity constant is a measure of the goodness of fit between a virus and a receptor and is important in determining, together with the number of receptors bound per virion, the effective or apparent affinity that governs the amount of virus binding to cells in equilibrium. Affinity constants have previously been measured for binding of purified influenza virus hemaglutinin to sialic acid (21). The kinetics of virus:receptor interactions are also of great importance, both because few processes reach equilibrium *in vivo*, and because the kinetic constants are of inherent interest and may lead to insights into the virus:host cell interaction and to useful comparisons with other receptor:ligand interactions. However, we are unaware of previous measurements of the kinetic constants for virus:receptor interactions. Binding of picornaviruses to soluble as well as cell surface receptors destabilizes these viruses and promotes disruption of the protein capsid and release of the viral RNA, which is thought to be important in the infection pathway (7, 19, 20, 22–24). Thermodynamic measurements of virus:receptor interaction may yield insights into the mechanism of destabilization.

To address these questions, we have applied surface plasmon resonance, using the BIAcore instrument (25), to the study of virus:receptor interactions (26). This technology has allowed us

* The costs of publication of this article were defrayed in part by the payment of page charges. This article must therefore be hereby marked "*advertisement*" in accordance with 18 U.S.C. Section 1734 solely to indicate this fact.

‡ To whom correspondence should be addressed: The Center for Blood Research, Harvard Medical School, 200 Longwood Ave., Boston, MA 02115.

[1] The abbreviations used are: ICAM-1, intercellular adhesion molecule-1; sICAM-1, soluble ICAM-1; IgSF, immunoglobulin superfamily; CHO, Chinese hamster ovary; MSX, L-methionine-sulfoximine; mAb, monoclonal antibody; PBS, phosphate-buffered saline; MES, 4-morpholineethanesulfonic acid; HRV3, human rhinovirus serotype 3.

to measure binding of soluble, monomeric ICAM-1 to rhinovirus, and dissociation from rhinovirus, in real time. The equilibrium constant derived from the kinetic constants, and direct measurement of the equilibrium constant by separation of the reactants by sedimentation, reveal two classes of sites that differ in affinity and association rate constant. There are dramatic differences in kinetic constants between binding of soluble ICAM-1 to rhinovirus and to mAb. The effect of lowered pH and receptor dimerization on kinetics and equilibria have been examined. Furthermore, we have determined the kinetic constants at different temperatures and found that heat is absorbed upon receptor binding, which has implications for destabilization of the virion in receptor-mediated disruption.

MATERIALS AND METHODS

sICAM-1—sICAM-1, the extracellular portion of ICAM-1 containing IgSF domains 1–5, was expressed from the mutant cDNA clone Y452E/F* (18) using a recombinant baculovirus in SF9 cells as described previously (22). For expression of sICAM-1 after co-amplification with glutamine synthetase (GS) (27), Y452E/F* was introduced into the unique *Xho*I-*Not*I site of PBJ5-GS (28), to produce pBJ5-GS/IC1–5D. A CHO cell mutant (CHO Lec3.2.8.1.) (29) with highly restricted glycosylation was transfected with PBJ5-GS/IC1–5D using calcium phosphate. After transfection, cells were grown in selective medium with 10% dialyzed serum. Selective medium was essentially as recommended (30) and contained minimum Eagle's medium without glutamine (Life Technologies, Inc.) supplemented with sodium pyruvate (Life Technologies, Inc.), minimum Eagle's medium-non-essential amino acid solution (Life Technologies, Inc.), glucose (0.3% final concentration), glutamic acid and asparagine (60 μg/ml), nucleosides (7 μg/ml), and L-methionine-sulfoximine (MSX). 25 μM MSX was used in the first round of selection. Clones secreting sICAM-1 to the extracellular medium were detected by enzyme-linked immunosorbent assay (31). After the first round of selection, clones were amplified using higher MSX concentrations (100 to 500 μM MSX). Clone CHO-ICAM-1(5D) 37.2.3.2 was seeded in roller bottles with expanded surface (Corning), and cells were grown to confluence using selective media (150 ml) containing 500 μM MSX and 10% dialyzed serum. Serum concentration was reduced to 5% when cells grew to confluence and the roller bottle maintained at 37 °C and 2 rpm for about 1 month. Medium was changed when the protein concentration was about 80 μg/ml as monitored by sandwich enzyme-linked immunosorbent assay.

sICAM-1 was purified from the cell supernatant by immunoaffinity chromatography with R6.5 mAb Sepharose as described (26), with the modification that size exclusion chromatography was with Sephadex G-200 in PBS, pH 8.0 (150 mM NaCl, 2.7 mM KCl, 1.47 mM KH_2PO_4, 4.86 mM Na_2HPO_4). Less nonspecific binding of sICAM-1 in BIAcore was found after purification at pH 8.0 than at pH 7.4. Protein concentration was determined from the extinction coefficient at 280 nm of 0.8 ml/mg cm (20). The molecular weight for the unglycosylated protein (49,600) was used to calculate molarity.

sICAM-1 expressed in baculovirus and mutant CHO cells has similar molecular weight (M_r) (~60,000) and glycosylation content (not shown). sICAM-1 differing in glycosylation had similar affinity for rhinovirus.[2]

IC1–5D/IgA was purified as described previously (20).

Virus Obtention—HRV3 was purified, washed free of bovine serum albumin, and concentration determined spectrophotometrically as described previously (22, 26).

Immobilization of Rhinovirus and Antibodies in BIAcore—HRV3 was covalently immobilized to the dextran surface of certified CM5 sensor chips via primary amino groups, using the amine coupling kit (Pharmacia Biosensor AB (26)). Briefly, carboxylate groups on the dextran were activated by injection of a mixture of *N*-hydroxysuccinimide and *N*-ethyl-*N'*-(dimethylaminopropyl)carbodiimide. Purified virus diluted with 10 mM sodium acetate, pH 5.7, was injected through the activated surface. Ethanolamine hydrochloride, pH 8.5, was injected after virus immobilization to block unreacted *N*-hydroxysuccinimide esters. Running buffer in BIAcore used for washing and the dissociation phase was PBS, pH 8.0, and was identical to the buffer that sICAM-1 was obtained in after Sephadex G-200 chromatography. After each cycle of sICAM-1 association and dissociation, HRV3 was regenerated with 3 pulses of 2 or 3 min of 25 mM MES buffer, pH 6.0, separated by about 1 min of PBS, pH 8.0. Polyclonal rabbit anti-mouse Fc γ antibody (Pharmacia) was immobilized (about 8,000 resonance units) using the amine coupling kit as recommended by the manufacturer.

Analysis of the Binding Data in BIAcore—Sensorgrams recorded during the interaction of sICAM-1 with immobilized virus or captured anti-ICAM-1 antibodies were analyzed by the linear transformation method to obtain the kinetic constants (32), using the equation $dRU/dt = k_a$ [sICAM-1] $RU_{max} - RU$ (k_a [sICAM-1] + k_d), where RU is resonance units. Linear analysis of the binding data uses the slope (k_s) of a plot of dRU/dt *versus* R to determine the association rate constant (k_a). The equation $k_s = k_a$ [sICAM-1] + k_d allows determination of k_a from a plot of k_s *versus* sICAM-1 concentration. Several sICAM-1 concentrations were required, as described in the figure legends.

Nonlinear curve fitting was carried out with the BIA evaluation 2.0 program, using models of one site or two independent sites to calculate association rate constants.

The portion of the sensorgram that corresponds to the dissociation of sICAM-1 from the rhinovirus or antibody surfaces was analyzed to obtain k_d. The slope of a plot of $\ln(R1/R_n)$ *versus* time yielded k_d, where $R1$ is the initial RU and R_n is RU with time. The sensorgrams obtained for the highest ligand concentration were analyzed to minimize rebinding during dissociation. When k_d was determined at different flow rates, no change was detected.

Saturation Binding of sICAM-1 to HRV3 in Solution—sICAM-1 was labeled with [^{35}S]methionine and cysteine, purified, and concentration determined by A_{280} as described (22). A mixture of labeled and unlabeled sICAM-1 (0.2–10 μM final concentration) was incubated with HRV3 (2.1×10^9 virions/μl) in 75 μl for 1 h at 20 or 15 °C, and 70 μl was subjected to sucrose gradient sedimentation for 1 h at 40,000 rpm at 4 °C and fraction collection and scintillation counting as described (22). sICAM-1 that sedimented with the virus in the region of 120–149 S, and input sICAM-1, were used to calculate the concentration of bound and free sICAM-1 in the 75-μl reaction mixture. No sedimentation of sICAM-1 was observed when virus was omitted or when R6.5 mAb to ICAM-1 was added.

RESULTS

Interaction of sICAM-1 with Immobilized Rhinovirus in BIAcore—Human rhinovirus serotype 3 (HRV3) was covalently coupled through amino groups to dextran that is immobilized on the gold film on the surface of the BIAcore sensor chip. Changes in density of the solution within the vicinity of the gold film (<1 wavelength) can be measured, because this affects the refraction of polarized light and the angle of the absorption maximum by the plasmon electrons of the gold film (25). The density in the vicinity of the gold film increases as virus is covalently immobilized, or ICAM-1 is noncovalently bound. Reactions occur within a 0.12-nl dextran layer on a sensor chip in a 60-nl flow chamber and are measured by the change in RU. About 10,000 RU of virus were typically covalently immobilized, corresponding to a concentration of 12.3 μM within the dextran layer and a total of 1.5 fmol. Specificity was examined by injecting ICAM-1 at 20 °C through flow chambers that contained dextran that was either covalently coupled to HRV3 or mock-coupled in the absence of HRV3 (Fig. 1*A*). sICAM-1 (6 μM) bound to immobilized HRV3 (454 RU), but little or no binding was obtained when no virus was present (36 RU). Binding of sICAM-1 (5 μM) to the viral surface was inhibited 85% when the sICAM-1 was preincubated with R6.5 monoclonal antibody (6 μM) for 15 min at 37 °C (not shown). Reproducible binding of sICAM-1 to immobilized HRV3 was obtained, and the virus remained intact as shown by binding of the same amount of sICAM-1 and no change in the base line after regeneration, for at least 12 successive cycles of binding and regeneration (26). Regeneration, *i.e.* dissociation of the bound sICAM-1 between successive cycles of injection of sICAM-1, was achieved at 20 °C with 3 pulses of 25 mM MES buffer, pH 6.0.

Determination of the association kinetic constant (k_a) requires measurement of association kinetics at several different sICAM-1 concentrations, whereas dissociation kinetics can be measured at all concentrations with typically the highest concentration yielding the most reproducible data; sensorgrams

[2] J. M. Casasnovas and T. A. Springer, unpublished results.

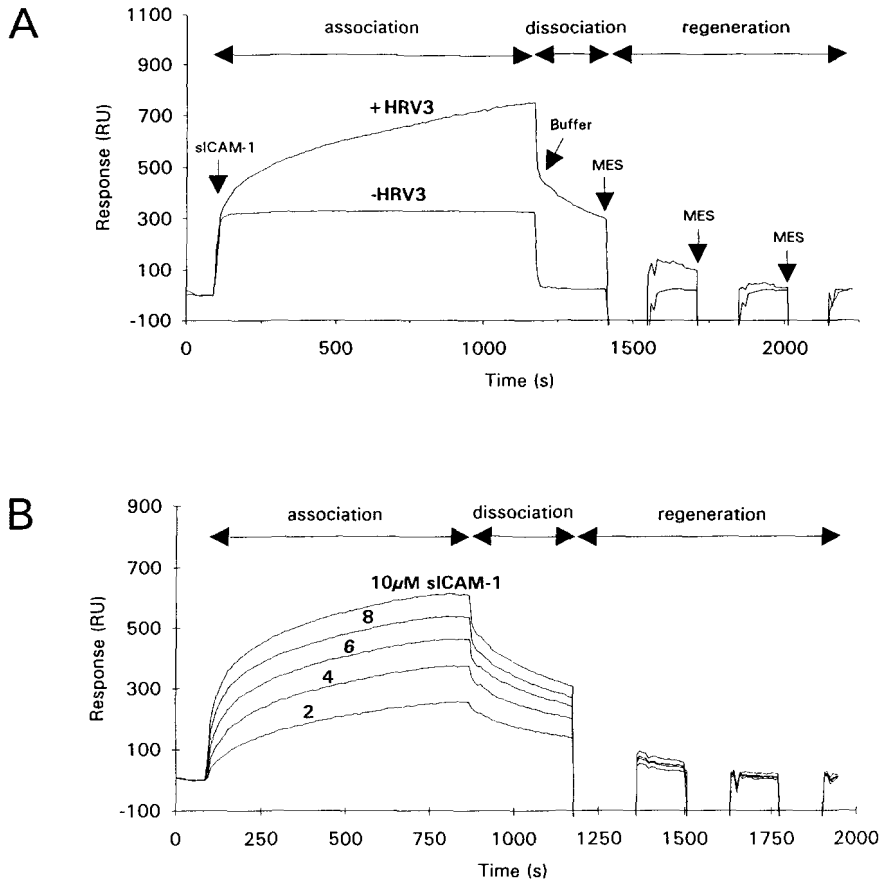

FIG. 1. **Sensorgrams recording interaction of sICAM-1 with rhinovirus in BIAcore.** Association during injection with sICAM-1 and dissociation during injection of buffer lacking sICAM-1 are marked by a gradual increase and decrease in resonance units (*RU*), respectively. Changes in buffer are marked by sharp changes in RU because of changes in buffer density. Regeneration in the final segments of the plots with pH 6.0 MES buffer occurs after 1400 or 1200 s and is marked by a return to the preinjection base line. *A*, overlay plot of sensorgrams, normalized to the same preinjection RU, recorded where sICAM-1 (6 μM) was injected at a flow rate of 2 μl/min and 20 °C through a carboxymethylated dextran surface that had been coupled without (−) or with (+) HRV3 (~10,000 RU). This was followed by an injection of PBS for 3.5 min. during which sICAM-1 dissociated from the surface. The matrix was then regenerated with three pulses (3 min) of 25 mM MES buffer, pH 6.0. *B*, overlay plot of sensorgrams obtained from successive cycles of association, dissociation, and regeneration. sICAM-1 (2, 4, 6, 8, and 10 μM) was successively injected through the sensor chip with immobilized rhinovirus at a flow rate of 3 μl/min at 20 °C. HRV3 was regenerated with 3 pulses (3, 2, and 2 min) of 25 mM MES buffer, pH 6.0.

showing association and dissociation obtained in a typical experiment are overlaid in Fig. 1*B*. The rate of ICAM-1 binding (dRU/d*t*) slowed during the association phase, but binding of sICAM-1 (RU) did not plateau, showing that equilibrium was not reached during the injection period. The HRV3 was stable during the experiment, because a very similar base line was recorded at the beginning and end of each cycle. The ratio of the maximal RU of bound sICAM-1 to the RU of covalently immobilized HRV3 was 0.075. Calculations using the M_r of virions (8.16×10^6) and sICAM-1 (60,000), and 60 binding sites per virion, yield binding of sICAM-1 that is 14–18% of the theoretical maximum and may indicate that this is the percentage of binding sites that are accessible or remain active after coupling to dextran.

Plots of the rate of association (dRU/d*t*) of sICAM-1 with HRV3 *versus* the amount of sICAM-1 that had associated (RU) were biphasic (Fig. 2*A*). Two classes of binding sites were distinguished by linear transformation of the data (Fig. 2*A*) and by nonlinear curve fitting (data not shown). The latter method yielded poor fits for one binding site ($\chi^2 = 45$) and excellent fits for two sites ($\chi^2 = 1.8$). Both the linear and nonlinear methods gave similar k_a values.

Interaction of sICAM-1 with immobilized mAb to ICAM-1 was measured for comparison to results with HRV3. The plot for the association of sICAM-1 with R6.5 mAb (and other mAb, data not shown) showed a single straight line (Fig. 2*B*).

The rates (k_s) for the first phase (Fig. 3*A*) and second phase (Fig. 3*B*) of association of sICAM-1 with HRV3 were plotted against sICAM-1 concentration. The slope of the line yielded k_a with a correlation coefficient $r > 0.99$. The intersection with the *y* axis is one method of determining k_d and yielded similar results for the first and second phases of association of 1.7×10^{-3} s^{-1} and 1.8×10^{-3} s^{-1}, respectively. Plots of k_s *versus* sICAM-1 concentration for association of sICAM-1 with mAb also yielded straight lines with $r = 0.99$.

Plots of dissociation of sICAM-1 from HRV3 *versus* time which have a slope = k_d yielded a straight line (Fig. 3*C*). No change in k_d was observed when the injection rate during dissociation was increased to 8 μl/min (not shown). Plots of dissociation of sICAM-1 from mAb were also linear and yielded k_d that did not change with injection rate. Invariance with injection rate for dissociation from HRV3 and mAb suggested there was no significant rebinding of dissociated sICAM-1.

Kinetic Rate Constants—The kinetic rate constants for sICAM-1 interaction with HRV3 were highly reproducible. Representative data obtained with four different HRV3 preparations and with four different preparations of sICAM-1 from CHO cells and insect cells are shown in Table I. The association rate constant for the first phase of association, $k_{a,1}$, was 2450 ± 300 M^{-1} s^{-1}. This is slow relative to other studied association rate constants, including mAb (see below). The rate for $k_{a,2}$ was 18-fold slower than for $k_{a,1}$. The k_d rate constant was $1.67 \times 10^{-3} \pm 0.1 \times 10^{-3}$ s^{-1}. The equilibrium dissociation constant (K_D) was calculated from k_d/k_a, using $k_{a,1}$ to obtain K_D1 and $k_{a,2}$ to obtain K_D2. These values were 0.69 ± 0.09 μM and 12.5 ± 1.2 μM, respectively.

The amount of binding to the two classes of sites was determined from the amount of bound sICAM-1 at the inflection point in the binding curves at high (near saturation) concentrations of sICAM-1 and also from Scatchard plots of the amount of binding to the two classes of sites. Both methods suggested that the sites with higher and lower k_a comprise about 40–50% and 50–60% of the total sites, respectively.

We obtained comparative kinetic data on three mAb that bind to ICAM-1. The mAb bind to sites on ICAM-1 overlapping or nearby to the site that binds HRV, since all three mAb block binding of HRV to rhinovirus (10), and the epitopes have been mapped to IgSF domains 1 or 2 (16) (Table II). The k_a of

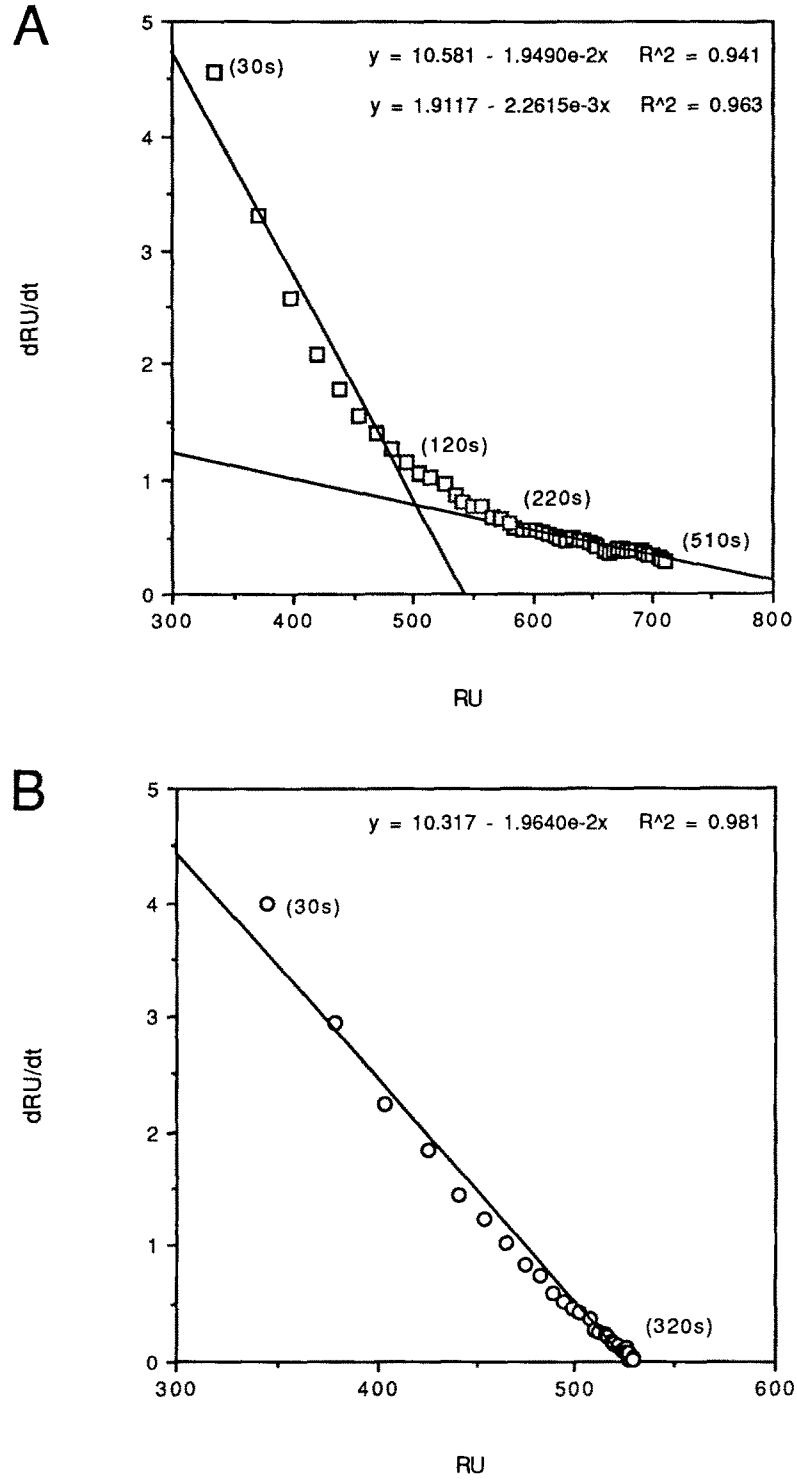

FIG. 2. **Linear transformation of the association of sICAM-1 with immobilized HRV3 and anti-ICAM-1 R6.5 mAb.** The value of dRU/d*t* every 10 s during the association phase was plotted *versus* RU. Selected time intervals after the beginning of the association with sICAM-1 are shown in *parentheses*. *A*, sICAM-1 (8 μM) was injected through a sensor chip with immobilized HRV3 at 3 μl/min and 20 °C as in Fig. 1*B*. *B*, R6.5 mAb to ICAM-1 (25 μg/ml) was injected for 12 min followed by sICAM-1 (1 μM) for 13 min in PBS at 20 °C and 3 μl/min through a sensor chip containing immobilized rabbit anti-mouse Fc antibody.

sICAM-1 for the three mAb was 17,000–47,800 M^{-1} s^{-1} or 7–20-fold faster than $k_{a,1}$ for HRV3. By contrast, the k_d values for HRV3 and the three mAb were quite similar.

Affinity in Solution—We compared our measurements with classical techniques for measuring affinity in solution. HRV3 (1.2 nM) was incubated with varying amounts of ^{35}S-sICAM-1 for 1 h at 20 or 15 °C, chilled on ice, and virus-bound sICAM-1 was separated from free sICAM-1 by sucrose gradient sedimentation at 4 °C. The Scatchard plot (Fig. 4) showed two classes of binding sites that differed in affinity. K_D1 and K_D2 determined from three independent experiments at 20 °C (±S.D.) were 0.55 ± 0.2 μM and 5.7 ± 2.0 μM, respectively. $K_{D,1}$ and $K_{D,2}$ at 15 °C were 0.84 μM and 6.9 μM. The high affinity sites comprised 48% of the total at both temperatures.

Effect of pH on the Interaction of sICAM-1 with Rhinovirus—Rhinoviruses are labile to pH lower than 6.0 (33). Lowering pH below 7.0 decreases the amount of sICAM-1 that associates with rhinovirus as shown by co-sedimentation in sucrose gradients (22). We tested the effect of lowered pH on the kinetics and equilibria of ICAM-1 binding to HRV3 (Table III). The affinity of HRV3 for sICAM-1 (inverse of $K_{D,1}$) was 1.8-fold lower at pH 7 than pH 8. A decrease from pH 7 to pH 6.5 resulted in a further 4.6-fold drop in affinity, primarily due to a 3.2-fold drop in $k_{a,1}$. At pH 6 there was a substantial further

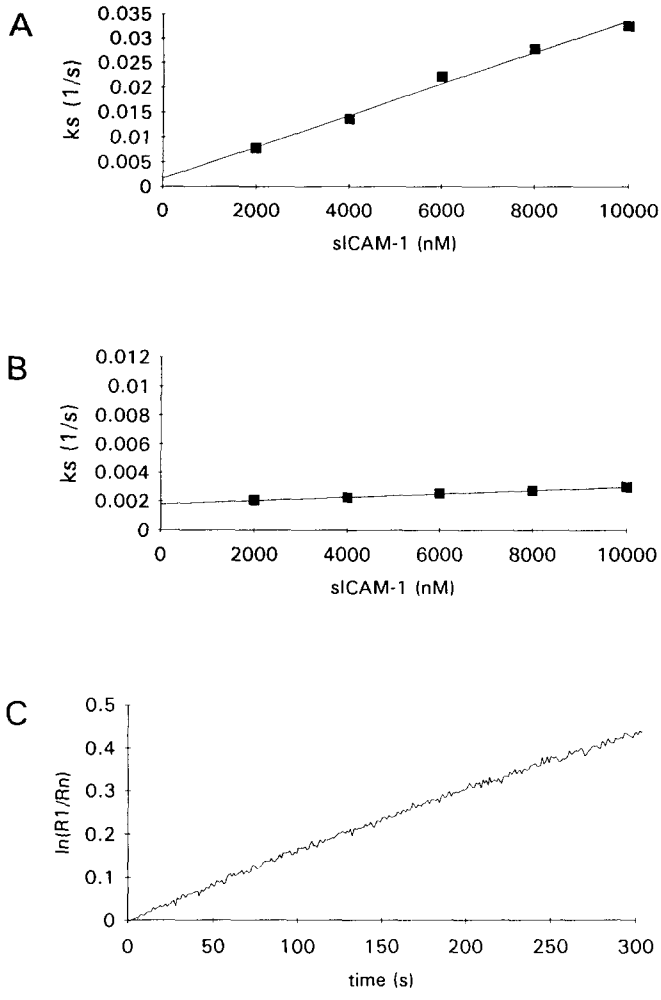

FIG. 3. **Representative plots for determination of the kinetic rate constants for sICAM-1 interaction with HRV3.** *A* and *B*, linear transformations of the association phase of sensorgrams as shown in Fig. 2*A* were used to obtain the slopes (k_s) from the first (*A*) and second (*B*) part of the association phase and k_s was plotted *versus* sICAM-1 concentration. The slope of these curves obtained by linear regression equals k_a. *C*, a representative linear transformation of the sensorgram from the dissociation phase obtained with 10 μM sICAM-1. *R1*, resonance units at beginning of dissociation; *Rn*, resonance units at the indicated time.

drop in affinity, as shown by less binding of sICAM-1 at the end of the association phase with 10 μM sICAM-1 than at higher pH (Table III). The k_d was 2-fold faster at pH 6.0 than at pH 6.5, and too little sICAM-1 was bound for measurement of k_a. The affinity roughly dropped 6-fold from pH 6.5 to 6.0, since the same amount of sICAM-1 was bound at the end of the association phase at pH 6.5 with 5 μM sICAM-1 (52 RU) as at pH 6.0 with 30 μM sICAM-1 (48 RU). Thus, from pH 8 to pH 6 there was a marked drop in affinity of approximately 50-fold. There was no disruption of HRV3 at pH 6 to 8 at 20 °C, since there was no change in the base line of immobilized rhinovirus, and since binding of sICAM-1 was reproducible in repeat experiments with the same sensor chip, and since full sICAM-1 binding activity was obtained in binding experiments at pH 8 that followed those at pH 6 (data not shown). Indeed, it should be noted that the ICAM-1 binding sites on HRV3 were routinely regenerated at the end of every association and dissociation cycle with pulses of pH 6 buffer.

Effect of ICAM-1 Dimerization on the Interaction with Rhinovirus—A dimeric ICAM-1 chimera, with ICAM-1 IgSF domains 1–5 fused to the hinge, CH2, and CH3 domains of the IgAI Fc region, has increased efficacy in neutralizing and disrupting rhinovirus (20); however, its affinity has not been measured previously. We measured the kinetics of the interaction of this IC1–5D/IgA chimera with HRV3 (Table IV). The kinetics were measured in terms of the concentration of the ICAM-1 moiety, *i.e.* for the dimeric chimera 2 × the molar concentration. The $k_{a,1}$ and $k_{a,2}$ kinetic constants were 1.6- and 2.8-fold faster for IC1–5D/IgA than for sICAM-1, respectively, whereas k_d was 7.6-fold slower. This resulted in a 17-fold higher affinity for IC1–5D/IgA than for sICAM-1.

Thermodynamics of the Interaction of sICAM-1 with HRV3 and R6.5 mAb—Thermodynamics of the interactions were determined by measuring kinetic constants at temperatures ranging from 10 to 25 °C (Table V and Fig. 5). For the interaction of sICAM-1 with both HRV3 and R6.5 mAb, k_a and k_d increased with increasing temperature. For HRV3, $k_{a,1}$ and $k_{a,2}$ increased more than k_d, whereas for R6.5 mAb k_a increased less than k_d. The data fit straight lines on Arrhenius plots (Fig. 5) except for the k_d for HRV3 at 25 °C. This value was disregarded in the plot because of decrease in the HRV3 RU base line at the end of each cycle at 25 °C, suggesting virus disruption; at 30 °C substantial disruption of HRV3 occurred in the presence of sICAM-1 (26). The $K_{D,1}$ and $K_{D,2}$ for HRV3 decreased by 1.2- and 1.4-fold as temperature increased from 10 to 20 °C. By contrast, the K_D for R6.5 mAb increased from 10 to 20 °C by 1.3-fold.

The activation energy (E_a) for association and dissociation was determined from Arrhenius plots (Fig. 5). The highest E_a were for $k_{a,2}$ for sICAM-1 binding to HRV3 and k_d for dissociation of sICAM-1 from R6.5 mAb. The E_a for dissociation of sICAM-1 was markedly higher with R6.5 mAb than with HRV3.

The enthalpy ($\Delta H°$) and free energy ($\Delta G°$) for the association of sICAM-1 with HRV3 and R6.5 at 20 °C were determined from the activation energies and affinity constants, respectively (Table VI). The HRV3-sICAM-1 interaction is an endothermic process, as shown by the positive $\Delta H°$ for the reaction. Association of sICAM-1 with the second class of binding sites on HRV3 was markedly more endothermic than with the first class. Association of sICAM-1 with R6.5 mAb was exothermic, with a negative $\Delta H°$. The entropy term ($T\Delta S°$) was positive for both interactions, but was higher for the interaction of sICAM-1 with HRV3 than with R6.5.

DISCUSSION

We have measured the kinetic constants for the interaction of a virus with its receptor. We adapted surface plasmon resonance to the study of virus-receptor interactions, and found it to be an accurate method for measuring kinetic constants, with standard deviations that were almost always less than 10% of the mean and with results that were highly reproducible with independent viral and receptor preparations. The utility of the method was enhanced by development of conditions that allowed at least 12 successive cycles of sICAM-1 binding and regeneration to be carried out with a single rhinovirus-sensor chip preparation (26). No disruption of the virus was detected in the determination of the kinetic and dissociation constants at 20 °C and below, as monitored by changes in the base line or amount of sICAM-1 bound.

The association rate constants for binding of sICAM-1 to HRV3 were low, 2450 and 130 M^{-1} s^{-1}. Since we are unaware of any previous measurements of the kinetic constants for virus binding to receptors, it is useful to compare kinetic measurements for other protein-protein interactions. Association rate constants for antibody binding to proteins in solution or on the cell surface range from 10^4 to 2×10^6 M^{-1} s^{-1} (34), consistent with our range of $2–5 \times 10^4$ M^{-1} s^{-1} for three ICAM-1 mAbs.

TABLE I

Kinetic and dissociation constants for sICAM-1 and HRV3

Four representative experiments are shown that used four different preparations of sICAM-1 (from insect cells in experiments 1 and 2 and from Lec 3.2.8.1 CHO cells in experiments 3 and 4) and four different preparations of HRV3. A range of concentrations of sICAM-1 from 1 to 10 μM was injected in each experiment as in Fig. 1*B*. $k_{a,1}$ and $k_{a,2}$ were obtained from the analysis of the first and second part of the biphasic association phase, respectively. Dissociation constants are the average of measurements from the dissociation phase of the two highest sICAM-1 concentrations. K_D were calculated from the kinetic constants; $K_{D,1} = k_d/k_{a,1}$ and $K_{D,2} = K_d/k_{a,2}$. Standard deviations are in parentheses.

	$k_{a,1}$	$k_{a,2}$	$k_d \times 10^3$	$K_{D,1}$	$K_{D,2}$
	$M^{-1}\ s^{-1}$		s^{-1}	μM	
Exp. 1	2,910	121	1.75	0.60	14.4
Exp. 2	2,420	131	1.50	0.62	11.4
Exp. 3	2,400	151	1.74	0.72	11.5
Exp. 4	2,063	132	1.70	0.82	12.8
Average	2,450 (300)	134 (11)	1.67 (0.1)	0.69 (0.09)	12.5 (1.2)

TABLE II

Kinetic and dissociation constants for sICAM-1 and mAb

A polyclonal rabbit anti-mouse Fc antibody (Pharmacia) was coupled to dextran in the sensor chip. Anti-ICAM-1 monoclonals (32 μl, 20 μg/ml) and sICAM-1 (36 μl; 50, 100, 150, 200, 250, or 300 nM) were consecutively injected through the surface containing the rabbit antibody for 8 and 9 min, respectively, at 4 μl/min at 25 °C in PBS, pH 8.0. The rabbit anti-mouse Fc was regenerated by injection of 8 μl of 100 mM HCl after each cycle. k_a is from a single or two experiments, with range in parenthesis. k_d is the average and s.d. of measurements from the dissociation phase from three cycles where 300, 500, and 750 nM sICAM-1 were injected at 4, 8, and 30 μl/min, respectively.

Antibody	Epitope	k_a	$k_d \times 10^3$	K_D
		$M^{-1}\ s^{-1}$	s^{-1}	nM
R6.5	Domain 2	23,700	1.83 (0.24)	77
LB2	Domain 1	17,100 (1,200)	1.79 (0.09)	105
RR1/1	Domain 1	47,800	1.80 (0.07)	38

On rates for the IgE receptor and insulin receptor are 6×10^4 and 3×10^6 M^{-1} s^{-1} (34), respectively, whereas the adhesion molecules CD2 and CD48 interact with an on rate $> 10^5$ M^{-1} s^{-1} (35). The latter interaction has an affinity similar to that of ICAM-1 for HRV3. There are two interesting possible explanations for why association of sICAM-1 with rhinovirus proceeds 1–2 orders of magnitude more slowly than typically found for protein:protein interactions. The location of the rhinovirus binding site in a depression in the viral capsid may make it relatively inaccessible and require precise orientation of the ICAM-1 for binding. Alternatively, there may be a requirement for a conformational change in the binding site on rhinovirus for ICAM-1 to bind.

The k_d of 1.67×10^{-3} s^{-1} found for sICAM-1 and HRV3 translates to a $t_{1/2}$ or lifetime of the receptor-ligand bond of 6.9 min. The k_d was not unusual and was similar to that found for three different mAb to ICAM-1.

We found two different kinetic association constants for the sICAM-1 interaction with rhinovirus. This contrasted with the results for association of three mAb with sICAM-1, where a single k_a was found. Of the binding sites on HRV3, 40–50% bound with the faster on rate and the remainder with the slower on rate. Using our kinetic constants, we calculated the equilibrium dissociation constant of sICAM-1 for HRV3. The K_D is 0.69 ± 0.09 μM and 12.5 ± 1.2 μM for the two classes of binding sites. Equilibrium binding measurements in solution yielded a biphasic Scatchard plot. The K_D of 0.55 ± 0.2 μM and 5.7 ± 2.0 μM were in good agreement with the BIAcore results. There were almost equal numbers of low and high affinity sites, as also found with BIAcore.

There are several possible explanations for the two classes of low and high affinity binding sites. One, there could be inherent differences between the structure of binding sites on the rhinovirus capsid. These two classes of binding sites appear to be on the same virion rather than on different classes of virions, because the rhinovirus sedimentation coefficient shifted gradually from 149 to 120 S as increasing amounts of sICAM-1 were added, and two different populations of virions that were altered in sedimentation by different concentrations of sICAM-1 were not seen (22). Binding of "pocket factor" to pockets underlying half of the sites could produce the observed heterogeneity (3). Two, binding of sICAM-1 could induce conformational changes in the rhinovirus capsid that alters the structure of neighboring binding sites. Three, binding of the first 2 or three molecules of sICAM-1 per pentamer might proceed without hindrance, but binding of further sICAM-1 molecules might be impeded. Electron microscopy of a two-domain fragment of ICAM-1 bound to rhinovirus reveals no contacts between neighboring ICAM-1 molecules (5); however, bound ICAM-1 projects outward from the virus and thus might kinetically hinder binding, by requiring more precise orientation for an ICAM-1 molecule to gain access to a neighboring binding site.

Our K_D measurements may be compared with previous determinations of the IC_{50} for inhibition by sICAM-1 of virus binding to cells, infection at high multiplicity of infection or plaque-forming units (7, 18, 20). For HRV3, the IC_{50} for inhibition of binding to purified ICAM-1 on a substrate was 3.5 μM, and the IC_{50} for infectivity at high MOI and in plaque-forming assays was 1.2 μM and 0.4–0.3 μM, respectively (7, 20). The high affinity K_D of 0.7 μM is close to these IC_{50} values and suggests that occupancy of these sites may be sufficient for inhibition of these processes. Inhibition of binding to cells is obtained at lower IC_{50} values of 45 nM (20), suggesting that occupancy of only a few sites is sufficient to inhibit virus attachment. IC_{50} values for HRV54 (18) and HRV14 (20) are lower than for HRV3, and these viruses may have correspondingly lower K_D for sICAM-1.

Multivalency results in an effective increase in affinity. Multivalent chimeric molecules containing IgSF domains 1–2 or 1–5 of ICAM-1 fused to Fc portions of IgA1 or IgM exhibited lower IC_{50} than sICAM-1 in assays of binding to cells, disruption, and plaque-forming units (20). We measured the kinetics and K_D for the IC1–5D/IgA chimera in units of concentration of the ICAM-1 moiety, for fair comparison with sICAM-1. The chimera, like sICAM-1, exhibited two k_a. The $k_{a,1}$ and $k_{a,2}$ were 1.6- and 2.8-fold faster than for sICAM-1, respectively. Theoretically, k_a for sICAM-1 and IC1–5D/IgA are predicted to be the same (34). Bivalent binding is predicted to result in a decreased k_d, in agreement with the finding that k_d was 7.5-fold lower for IC1–5D/IgA than for sICAM-1. The K_D for IC1–5D/IgA were 50 and 411 nM, 17-fold lower than for sICAM-1. This compares with IC_{50} values for IC1–5D/IgA of 7.5-, 12.6-, or 187-fold lower than for sICAM-1 for virus binding, disruption, or plaque-forming units, respectively (20). The IC_{50} values for these three assays were 1.6–38 nM. Compared with the high affinity K_D of 50 nM or average K_D of 230 nM, this suggests that 50% inhibition occurs when substantially less than 50% of the

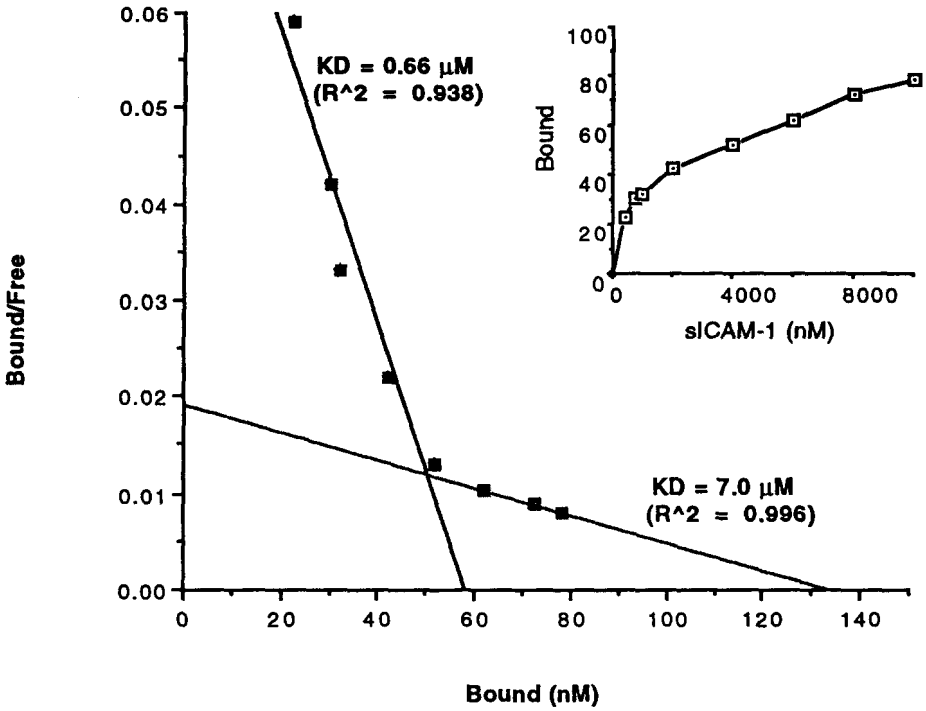

FIG. 4. **Equilibrium binding of sICAM-1 to HRV3 in solution.** HRV3 (2.1×10^9 virions/μl) was incubated with varying concentrations of ^{35}S-sICAM-1 for 60 min at 20 °C, chilled on ice, subjected to sucrose gradient sedimentation, and fractions were scintillation counted. Radioactivity that co-sedimented with the virus was used to calculate bound sICAM-1.

TABLE III

Effect of pH on kinetic and dissociation constants for sICAM-1 and HRV3

Kinetic association constants (k_a) are averages of two experiments with range in parentheses; k_d constants are average of four measurements with S.D. in parentheses. The buffer for injection of ICAM-1 and the dissociation phase was PBS adjusted to the indicated pH. sICAM-1 was at a range of concentrations from 1 to 10 μM, pH 8.0; 1 to 15 μM, pH 7.0; 5 to 30 μM, pH 6.5; and 10 to 30 μM, pH 6.0. $k_{a,1}$, $k_{a,2}$, and k_d were determined and K_D calculated as described in Table I. The last column shows the amount of sICAM-1 that was bound in RU after 13 min of injection at 10 μM. The amount of HRV3 immobilized was 11,000 RU.

pH	$k_{a,1}$	$k_{a,2}$	$k_d \times 10^3$	$K_{D,1}$	$K_{D,2}$	Bound sICAM-1 at 10 μM
	$M^{-1}\ s^{-1}$		s^{-1}	μM		RU
8.0	2,320 (260)	156.3 (24)	1.56 (0.14)	0.67	10.0	353
7.0	1,880 (83)	127.6 (3.9)	2.32 (0.06)	1.23	18.2	214
6.5	580 (200)	ND[a]	3.26 (0.26)	5.60	ND	66
6.0	ND	ND	6.00 (0.06)	ND	ND	32

[a] ND, not determined.

TABLE IV

Kinetic and dissociation constants for sICAM-1 and IC1–5D/IgA

Association rate constants were determined from two different experiments for each molecule using different sensor chips, as described in the legend to Fig. 1*B*. Measurement units are the concentration of ICAM-1 sites, *i.e.* 2 × molar concentration for IC1–5D/IgA. Concentrations injected ranged from 1 to 8 μM for sICAM-1 and 0.5 to 4 μM for IC1–5D/IgA. The experiments were done in parallel at 4 μl/min using PBS, pH 8.0. Dissociation constants were determined from the two highest protein concentrations in each experiment, and one additional experiment with the highest protein concentration at 10 μl/min. The standard deviation is in parentheses.

Sample	$k_{a,1}$	$k_{a,2}$	$k_d \times 10^3$	$K_{D,1}$	$K_{D,2}$
	$M^{-1}\ s^{-1}$			nM	
sICAM-1	2,690 (150)	189 (5.5)	1.67 (0.3)	621	8820
IC1–5D/IgA	4,410 (330)	538 (20)	0.221 (0.02)	50.1	411

sites/virion are occupied. The K_D for binding of HRV14 and HRV15 to HeLa cells is in the range of 10^{-11} M (6). Comparisons with our values of about 10^{-6} M and 10^{-7} M for monovalent and bivalent receptor binding clearly suggest that binding of HRV to cells is highly multivalent.

Both acidic pH and binding to receptor can cause disruption of rhinovirus and may be important in the pathway of infection. However, the combination of lowered pH and receptor binding are not synergistic and not even additive in disruption assays, and less sICAM-1 binding to HRV3 is seen at pH 6 than at pH 7 (19, 22). The affinity of sICAM-1 for HRV3 decreased 8-fold when pH was dropped from 8 to 6.5, primarily as a result of a drop in k_a. This is a very dramatic change in affinity over a small change around neutral pH and may suggest either a charged residue such as histidine that is important in binding or a cooperative change in capsid conformation that affects the receptor binding site.

The thermodynamics of ICAM-1 interaction with rhinovirus may have important implications for virus disruption. Most protein:protein interactions, *e.g.* antibody binding to protein antigens, are exothermic (negative ΔH) and thus have higher affinity as the temperature is decreased (34). The interaction of R6.5 mAb with sICAM-1 was an example of this. By contrast, interaction of HRV3 with ICAM-1 was endothermic; *i.e.* heat was absorbed by the sICAM-1-HRV3 complex. Both interaction with R6.5 mAb and HRV3 resulted in an increase in entropy, consistent with a hydrophobic interaction that results in increased disorder of water molecules. We have previously meas-

TABLE V

Kinetic and association constants for HRV3-sICAM-1 interaction at four different temperatures

sICAM-1 (1–10 or 1–12 μM) was injected at each temperature as shown in Fig. 1*B* and kinetic constants determined as described in Table I. Range (k_a) or standard deviation (k_d) are shown in parentheses.

Temperature	$k_{a,1}$	$k_{a,2}$	$k_d \times 10^3$	$K_{D,1}$	$K_{D,2}$
°C	$M^{-1}\ s^{-1}$		s^{-1}	μM	
10	1,620 (12)	80.5 (15.9)	1.31 (0.19)	0.81	16.27
15	1,960 (80)	110.5 (3.2)	1.42 (0.14)	0.72	12.85
20	2,410 (8)	141.2 (10.2)	1.61 (0.13)	0.67	11.40
25	3,000 (100)	195.4 (5.8)	2.22 (0.14)	0.74	11.36

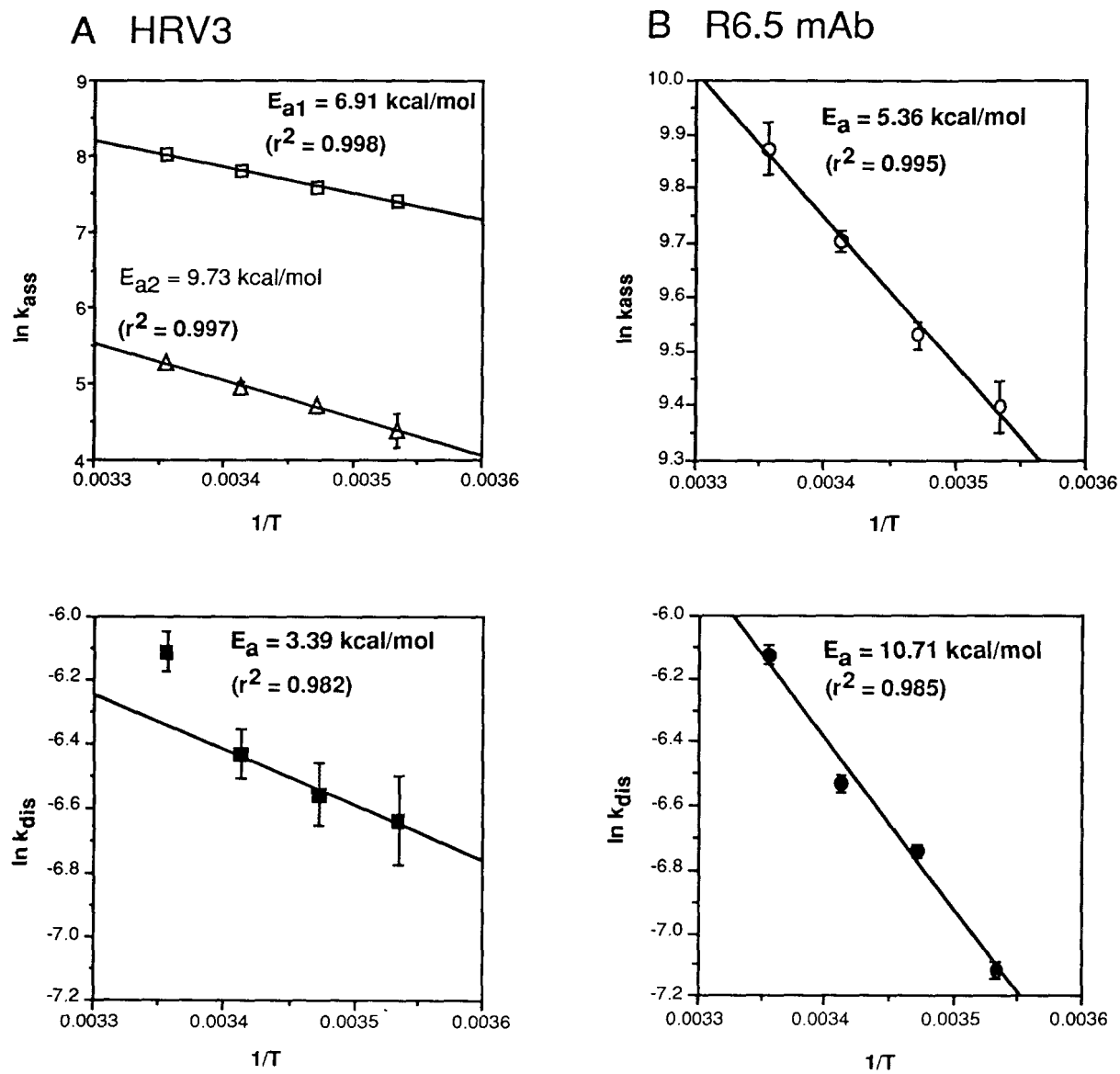

FIG. 5. **Activation energy for k_a and k_d.** Kinetic constants were determined in the BIAcore machine equilibrated to 10, 15, 20, or 25 °C. *A*, for HRV3 association, kinetic constants were determined using ICAM-1 concentrations of 1–12 μM and dissociation constants were determined using the two highest concentrations. Plots obtained with the kinetic constants determined for the first (*open squares*) and second phase (*open triangles*) of the association of sICAM-1 with HRV3 are shown. The mean and range are shown for two independent experiments. *B*, for R6.5 mAb, constants were determined as described in Table II in three different experiments where sICAM-1 was injected at 1, 2, or 4 μl/min through sensor chips with about 900 RU of R.6.5 mAb captured with anti-mouse Fc. Nine concentrations of sICAM-1 between 100 and 500 nM were used in each experiment. k_d was determined from the sensorgrams obtained when sICAM-1 was injected at 350, 400, 450, and 500 nM at flow rate of 4 μl/min. Mean and S.D. are shown for three experiments (k_a) and four dissociations (k_d). Activation energy is obtained from the slope of the plots and *T* is in Kelvin.

ured the activation energy for disruption of rhinovirus as ~42 kcal/mol (22). Binding of sICAM-1 to rhinovirus accelerates the rate of disruption, and thus partially destabilizes the virion. Part of the heat absorbed when sICAM-1 is bound may contribute to lowering the activation barrier for disruption. The enthalpy for binding to the sites with slower k_a of 6.3 kcal/mol is substantially higher than for binding to sites with faster k_a of 3.5 kcal/mol. Binding to the former class of sites would be predicted to make a greater contribution to disruption because of the greater enthalpy. Since there are a total of 60 sites/

TABLE VI
Thermodynamic parameters

$\Delta H°$ was obtained from the difference between the activation energy for the association and dissociation reaction, which is equivalent to the activation energy for the equilibrium association constant. $\Delta G°$ was determined from the affinity constants at 20 °C ($\Delta G° = -RT \ln K_{eq}$), and $T\Delta S°$ was calculated from the difference between $\Delta H°$ and $\Delta G°$. Data from the first (1) and second (2) phase of the association of sICAM-1 with HRV3 are shown.

Interaction	$\Delta H°$	$\Delta G°$	$T\Delta S°$	$\Delta S°$
	kcal/mol			*cal/°K mol*
ICAM-1 and HRV3 (1)	3.5	−8.3	11.8	40
ICAM-1 and HRV3 (2)	6.3	−6.6	13.0	44
ICAM-1 and R6.5 mAb	−5.4	−9.4	4.0	14

virion, occupation of only a fraction of them would result in an increase in enthalpy similar to that of the activation energy of 42 kcal/mol. It may be significant that binding to the sites with lower enthalpy would precede kinetically binding to the sites with higher enthalpy; this may be important in the pathway of virus disruption and infection. Studies of virus disruption in BIAcore may lead to further insights into the physicochemistry of this process.

REFERENCES

1. Rossmann, M. G., Arnold, E., Erickson, J. W., Frankenberger, E. A., Griffith, J. P., Hecht, H. J., Johnson, J. E., Kamer, G., Luo, M., Mosser, A. G., Rueckert, R. R., Sherry, B., and Vriend, G. (1985) *Nature* **317,** 145–153
2. Kim, S., Smith, T. J., Chapman, M. S., Rossmann, M. G., Pevear, D. C., Dutko, F. J., Felock, P. J., Diana, G. D., and McKinlay, M. A. (1989) *J. Mol. Biol.* **210,** 91–111
3. Oliveira, M. A., Zhao, R., Lee, W.-M., Kremer, M. J., Minor, I., Rueckert, R. R., Diana, G. D., Pevear, D. C., Dutko, F. J., McKinlay, M. A., and Rossmann, M. G. (1993) *Structure* **1,** 51–68
4. Rossmann, M. G. (1989) *J. Biol. Chem.* **264,** 14587–14590
5. Olson, N. H., Kolatkar, P. R., Oliveira, M. A, Cheng, R. H., Greve, J. M., McClelland, A., Baker, T. S., and Rossmann, M. G. (1993) *Proc. Natl. Acad. Sci. U. S. A.* **90,** 507–511
6. Colonno, R. J., Condra, J. H., Mizutani, S., Callahan, P. L., Davies, M., and Murcko, M. A. (1988) *Proc. Natl. Acad. Sci. U. S. A.* **85,** 5449–5453
7. Greve, J. M., Forte, C. P., Marlor, C. W., Meyer, A. M., Hoover-Litty, H., Wunderlich, D., and McClelland, A. (1991) *J. Virol.* **65,** 6015–6023
8. Smith, T. J., Olson, N. H., Holland Cheng, R., Liu, H., Chase, E. S., Ming Lee, W., Leippe, D. M., Mosser, A. G., Rueckert, R. R., and Baker, T. S. (1993) *J. Virol.* **67,** 1148–1158
9. Greve, J. M., Davis, G., Meyer, A. M., Forte, C. P., Yost, S. C., Marlor, C. W., Kamarck, M. E., and McClelland, A. (1989) *Cell* **56,** 839–847
10. Staunton, D. E., Merluzzi, V. J., Rothlein, R., Barton, R., Marlin, S. D., and Springer, T. A. (1989) *Cell* **56,** 849–853
11. Tomassini, J. E., Graham, D., DeWitt, C. M., Lineberger, D. W., Rodkey, J. A., and Colonno, R. J. (1989) *Proc. Natl. Acad. Sci. U. S. A.* **86,** 4907–4911
12. Simmons, D., Makgoba, M. W., and Seed, B. (1988) *Nature* **331,** 624–627
13. Staunton, D. E., Marlin, S. D., Stratowa, C., Dustin, M. L., and Springer, T. A. (1988) *Cell* **52,** 925–933
14. Springer, T. A. (1995) *Annu. Rev. Physiol.* **57,** 827–872
15. Berendt, A. R., Simmons, D. L., Tansey, J., Newbold, C. I., and Marsh, K. (1989) *Nature* **341,** 57–59
16. Staunton, D. E., Dustin, M. L., Erickson, H. P., and Springer, T. A. (1990) *Cell* **61,** 243–254
17. McClelland, A., DeBear, J., Yost, S. C., Meyer, A. M., Marlor, C. W., and Greve, J. M. (1991) *Proc. Natl. Acad. Sci. U. S. A.* **88,** 7993–7997
18. Marlin, S. D., Staunton, D. E., Springer, T. A., Stratowa, C., Sommergruber, W., and Merluzzi, V. (1990) *Nature* **344,** 70–72
19. Hoover-Litty, H., and Greve, J. M. (1993) *J. Virol.* **67,** 390–397
20. Martin, S., Casasnovas, J. M., Staunton, D. E., and Springer, T. A. (1993) *J. Virol.* **67,** 3561–3568
21. Sauter, N. K., Bednarski, M. D., Wurzburg, B. A., Hanson, J. E., Whitesides, G. M., Skehel, J. J., and Wiley, D. C. (1989) *Biochemistry* **28,** 8388–8396
22. Casasnovas, J. M., and Springer, T. A. (1994) *J. Virol.* **68,** 5882–5889
23. Kaplan, G., Freistadt, M. S., and Racaniello, V. R. (1990) *J. Virol.* **64,** 4697–4702
24. Yafal, A. G., Kaplan, G., Racaniello, V. R., and Hogle, J. M. (1993) *Virology* **197,** 501–505
25. Malmqvist, M. (1993) *Nature* **361,** 186–187
26. Casasnovas, J. M., Reed, R. R., and Springer, T. A. (1994) *Methods: A Companion to Methods in Enzymology* **6,** 157–167
27. Davis, S. J., Ward, H. A., Puklavec, M. J., Willis, A. C., Williams, A. F., and Barclay, A. N. (1990) *J. Biol. Chem.* **265,** 10410–10418
28. Gastinel, L. N., Simister, N. E., and Bjorkman, P. J. (1992) *Proc. Natl. Acad. Sci. U. S. A.* **89,** 638–642
29. Stanley, P. (1989) *Mol. Cell Biol.* **9,** 377–383
30. Bebbington, C. R., and Hentschel, C. C. G. (1987) in *DNA Cloning: A Practical Approach* (Glover, D. M., ed) Vol. III, pp. 163–188, IRL Press, Oxford
31. Rothlein, R., Mainolfi, E. A., Czajkowski, M., and Marlin, S. D. (1991) *J. Immunol.* **147,** 3788–3793
32. Karlsson, R., Michaelsson, A., and Mattson, L. (1991) *J. Immunol. Methods* **145,** 229–240
33. Rueckert, R. R. (1990) in *Virology* (Fields, B. N., Knipe, D. M., Chanock, R. M., Hirsch, M. S., Melnick, J. L., Monath, T. P., and Roizman, B., eds) pp. 507–547, Raven Press, Ltd., New York
34. Mason, D. W., and Williams, A. F. (1986) in *Handbook of Experimental Immunology: Immunochemistry* (Weir, D. M., ed) Vol. 1, pp. 38.1–38.17, Blackwell Scientific Publications, Oxford
35. van der Merwe, P. A., Brown, M. H., Davis, S. J., and Barclay, A. N. (1993) *EMBO J.* **12,** 4945–4954